

## Liquid-Phase Boriding of High-Chromium Steel

Yu. F. Ivanov<sup>a, \*</sup>, V. E. Gromov<sup>b, \*\*</sup>, D. A. Romanov<sup>b, \*\*\*</sup>, O. V. Ivanova<sup>c, \*\*\*\*</sup>, and A. D. Teresov<sup>a, \*\*\*\*\*</sup>

<sup>a</sup>Institute of High Current Electronics, Siberian Branch, Russian Academy of Sciences, Tomsk, 634055 Russia

<sup>b</sup>Siberian State Industrial University, Novokuznetsk, Kemerovo oblast, Kuzbass, 654007 Russia

<sup>c</sup>Tomsk State University of Architecture and Building, Tomsk, 634003 Russia

\*e-mail: yufi55@mail.ru

\*\*e-mail: gromov@physics.sibsiu.ru

\*\*\*e-mail: romanov\_da@physics.sibsiu.ru

\*\*\*\*e-mail: dekanat\_oof@tsuab.ru

\*\*\*\*\*e-mail: tad514@yandex.ru

Received September 30, 2019; revised October 22, 2019; accepted November 15, 2019

**Abstract**—The structural-phase states and tribological properties of 12Kh18N10T steel subjected to electro-explosive alloying (EPA) with titanium and boron and subsequent electron-beam processing in various modes in terms of the energy density of the electron beam and the duration of the exposure pulse have been analyzed using methods of modern physical materials science. It has been established that EPA of steel with titanium and boron leads to the formation of a surface layer with multiphase submicro-nanocrystalline structure, characterized by the presence of micropores, microcracks, and microcraters. Complex processing, combining EPA and subsequent irradiation with high-intensity pulsed electron beams, leads to the formation of 60- $\mu\text{m}$ -thick multiphase submicro-nanocrystalline surface layer. It is shown that the phase composition of a surface layer of steel is determined by the mass ratio of titanium and boron during electroexplosive alloying. The microhardness of a modified layer is defined by the relative mass fraction of titanium borides in the surface layer and can be more than 18 times higher than the microhardness of steel in its initial state (before electroexplosive alloying). Modes of complex processing have been determined at which the surface layer containing exclusively titanium borides and intermetallic compounds based on titanium and iron is formed. The maximum (approximately 82% by weight) titanium boride content is observed when steel is processed in a regime with the highest mass of boron powder in the sample ( $m_B = 87.5$  mg;  $m_{Ti}/m_B = 5.202$ ). With a decrease in mass of boron powder, the relative content of borides in the surface layer of steel decreases. It was found that integrated processing of steel is accompanied by a sevenfold increase in microhardness of the surface layer and wear resistance of the steel increases by more than nine times.

**Keywords:** high-chromium stainless steel, boron, titanium, electric explosive alloying, intense pulsed electron beam, structure, properties

**DOI:** 10.3103/S0967091220070062

### INTRODUCTION

Conversion of nuclear power plants to more enriched fuel and, accordingly, strengthening the requirements for the absorption ability of materials shows a clear need for an increase in the boron concentration in steels, which are often employed in the fabrication of spent-fuel pools due to the high neutron absorbing ability of boron [1]. The maximum concentration of boron in recently used steels is less than 1.8 wt % (ChS82 steel), which is caused by low plasticity of boron-alloyed material due to the coarse shape of borides [2, 3]. Dispersion of the steel structure and spheroidization of borides are performed through thermomechanical treatment of steel [4] and additional alloying [5–9]. The cited methods and approaches are based on modification of the structure

and properties of bulk steel. In recent decades, methods for the modification of steel based on concentrated energy fluxes have been extensively used [10–16]. Electroexplosive alloying (EPA), which melts the treated surface by saturating the melt with the components of a plasma jet formed from the products of electroexplosion of a conductor, is one of these methods [17–19]. A number of studies have shown that additional irradiation of a material doped by an electroexplosive method with an intense pulsed electron beam promotes homogenization of the modified layer, removal of micropores and microcraters, and an increase in the mechanical, tribological and fatigue properties of part of a whole [20].

The aim of this study is to analyze the results and determine formation features of the structure and characteristics of austenite stainless high-chromium

steel exposed to alloying with titanium and boron using an integrated method, which combines saturation of the surface layer of the material with plasma of electroexplosion of an electrically conducting material and irradiation with a high-intense pulsed electron beam in the high-speed fusion mode and crystallization of the alloyed layer.

## MATERIAL AND METHODS OF TREATMENT AND PROCEDURES OF STUDY

Stainless 12Kh18N10T steel was used as the material of study [21]. The specimens appeared as plates  $10 \times 10 \times 5$  mm in size. The surface layer of the steel was alloyed using electroexplosive annealing (EPA) on an EVU 60/10 [17]. Foil of technically pure VT1-0 titanium, on the surface of which there was boron powder, was used as an electrically conducting material. The powder of V-99V-TU 1-92-1549 amorphous boron,  $B > 99\%$ , with a particle diameter of  $0.5\text{--}5.0$   $\mu\text{m}$  was used. The following parameters of EPA were used: the particle density was  $2.2$   $\text{GW}/\text{m}^2$  and the plasma pulse duration was  $100$   $\mu\text{s}$ . Four EPA modes were used, which are characterized by different titanium foil-to-amorphous boron powder mass ratio. The Titanium foil  $m_{\text{Ti}}$  to amorphous boron  $m_{\text{B}}$  mass ratios employed for EPA of 12Kh18N10T steel are given below:

Mode	$m_{\text{Ti}}$ , mg	$m_{\text{B}}$ , mg	$m_{\text{Ti}}/m_{\text{B}}$
1	360.7	50.0	7.214
3	392.2	62.5	6.275
5	423.7	75.0	5.649
7	455.2	87.5	5.202

In the second stage, the surface of some specimens modified with the electroexplosion method, was irradiated with a high-intensity pulsed electron (HIPE) beam [20] using the following parameters: the energy of accelerated electrons was  $17$  keV, the electron beam energy density was  $40$  and  $20$   $\text{J}/\text{cm}^2$ , the electron beam pulse duration was  $200$  and  $50$   $\mu\text{s}$ , and the number of pulses was  $3$ . Irradiation of the specimens with an electron beam was carried out twice. Firstly, the surface was irradiated with an electron beam with the parameters of  $17$  keV,  $40$   $\text{J}/\text{cm}^2$ ,  $200$   $\mu\text{s}$ , and  $3$  pulses; and, then,  $17$  keV,  $20$   $\text{J}/\text{cm}^2$ ,  $50$   $\mu\text{s}$ , and  $3$  pulses. The specimens were irradiated in integrated vacuum space using SOLO equipment [11]. The choice of the irradiation mode was based on the modeling results of the temperature field [22]. Thus, two stocks of specimens were studied, more specifically, specimens after EPA (further identified as specimens 1, 3, 5, and 7) and specimens after two-stage treatment with EPA + HIPE (further identified as specimens 2, 4, 6, and 8, where specimen 2 is the specimen exposed to EPA according to mode 1 and HIPE, while specimen 4 is

the specimen exposed to EPA according to mode 3 and HIPE, and so on).

Investigations of the steel structure in the initial state and after modification were carried out using X-ray analysis (an XRD 6000 diffractometer), as well as scanning (an SEM 515 Philips instrument) and transmission diffraction (a JEM-2100F) electron microscopy. Elemental analysis of the specimens was performed using X-ray microanalysis. The following characteristics of the modified layer were analyzed: microhardness (DUH-211S (Shimadzu, Japan), the load on the indenter corresponds to  $30$  mN, and PMT-3 instruments, the load on indenter was  $1$  N) and wear resistance (TRIBOtechnik instrument; dry friction condition at room temperature, countersolid is represented by a ShKh15 ball that was  $6$  mm in diameter, the track diameter was  $4$  mm, the rotation speed of the specimen was  $2.5$  cm/s, the load on the indenter was  $10$  N, and the number of turns was  $8000$ ). The wear resistance of the surface layer of material was calculated after profilometry of the formed track.

## RESULTS AND DISCUSSION

Electroexplosive treatment of 12Kh18N10T steel is accompanied by the formation of a highly developed pattern with a large number of microdrops, microcraters, microcracks, and metal flows, which is intrinsic for this method of exposure on the surface of metals and alloys (Fig. 1a). Subsequent irradiation of the modified steel with an intense pulsed electron beam is accompanied by smoothening of the material surface due to application of surface tension of melt and microcraters and metal flows disappear almost completely; however, a small number of microcracks remains (Fig. 1b).

The elemental composition of the modified layer of steel was determined using X-ray microanalysis [23]. Results of the studies are given in Fig. 2a. It should be noted that boron and titanium represent the main elements of the surface layer of the specimens after EPA (Fig. 2; modes 1, 3, 5, and 7) and the elements forming steel are present at marginal quantities. Consequently, electroexplosive annealing using the parameters chosen for this study was accompanied by the formation of not only an alloyed layer of steel, but also a thin coating based on titanium and boron. The maximum total concentration of boron and titanium atoms is detected in the surface layer of steel modified with the electroexplosion method according to modes 1 and 7. An increase in the relative content of boron powder in the sprayed shot (at successive change of modes  $1 \rightarrow 3 \rightarrow 5 \rightarrow 7$ , Fig. 2a) is accompanied by monotonous change in the concentration of boron in the alloyed layer.

Irradiation of the alloyed layer using HIPE is accompanied by the liquid-phase mixing of the surface layer of the material. This is indicated by a significant increase of the elements forming steel in the sur-

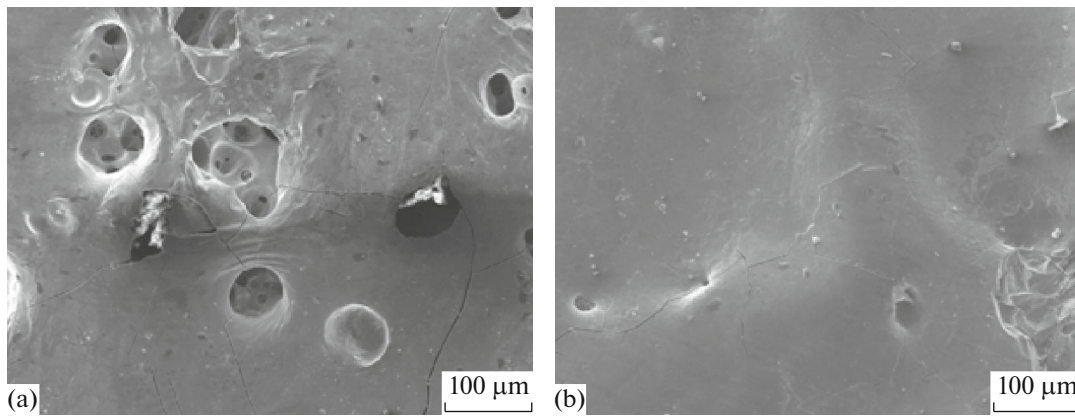


**Fig. 1.** Electron microscopic image of a steel surface structure after (a) electroexplosive alloying (EPA) using mode 3 and (b) subsequent irradiation by a high-intensity pulsed electron (HIPE) beam. Scanning electron microscopy.

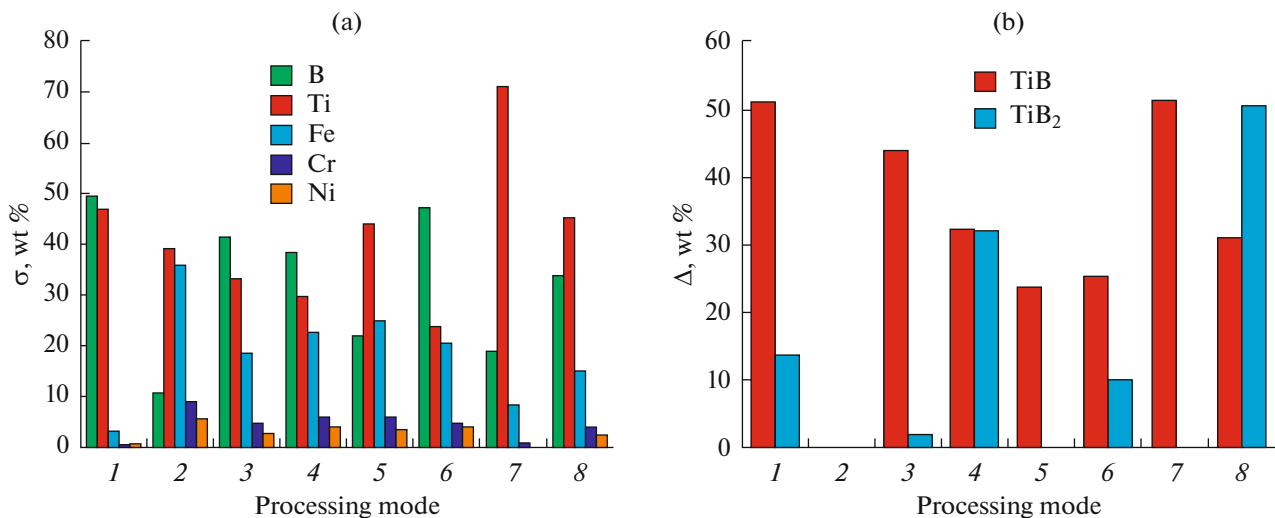


**Fig. 2.** Results of (a) X-ray microspectral and (b) X-ray phase analysis of the surface layer of 12Kh18N10T steel subjected to EPA with titanium and boron (at processing modes 1, 3, 5, 7) and subsequent HIPE irradiation (at processing modes 2, 4, 6, 8).

face layer (iron, chromium, and nickel) (Fig. 2a). However, it should be noted that the concentration of the main elements of a substrate in the surface layer monotonously decreases with an increase in the relative content of boron powder in the sprayed shot (at successive change of modes 2 → 4 → 6 → 8, Fig. 2a). The maximum concentration of boron in the surface layer of steel was determined in the specimen modified according to mode 6 (Fig. 2a).

Phase composition of the modified layer of steel was investigated using X-ray analysis. It was determined that electroexplosive annealing is accompanied by the formation of a multi-phase state in the surface layer, whose main phases are represented by titanium borides of TiB and TiB<sub>2</sub> composition (Fig. 2b). The maximum content of titanium borides in total achieving 75 wt % is formed upon electroexplosive annealing

according to mode 1 (Fig. 2b). In this case, the main titanium boride is TiB (Fig. 2b).

Subsequent irradiation of the modified layer of steel using HIPE results in a significant increase in the relative content of titanium diboride TiB<sub>2</sub>. This compound becomes the main phase in the surface layer of the specimen exposed to EPA according to mode 7 and further treatment using HIPE (Fig. 2b, mode 8). It can be suggested that an increase in the relative content of titanium diboride is caused by a significant difference in the temperatures of crystallization of these compounds; titanium diboride is formed at 3225°C and titanium boride is formed at 2200°C [24].

Mechanical characteristics of the surface layer of steel modified with EPA was characterized by microhardness (Table 1). Analyzing the results, it should be noted that EPA is accompanied by a manifold (5.2–8.1)

**Table 1.** Microhardness ( $HV$ ), wear coefficient ( $k$ ) and friction coefficient ( $\mu$ ) of 12X18H10T steel after EPA and additional HIEB exposure (EPA + HIEB)

Parameter	Mode							
	1	2	3	4	5	6	7	8
	EPA	EPA + HIEB						
$HV$ , MPa	35398.4	12891.0	10243.4	10866.0	11144.0	13763.0	18993.9	9398.0
$k$ , mm <sup>3</sup> /N m		$1.3 \times 10^{-3}$		$1.3 \times 10^{-3}$		$0.3 \times 10^{-3}$		$1.2 \times 10^{-3}$
$\mu$		0.61		0.57		0.65		0.60

For initial steel  $HV = 1952$  MPa;  $k = 2.8 \times 10^{-3}$  mm<sup>3</sup>/N m;  $\mu = 0.58$ .

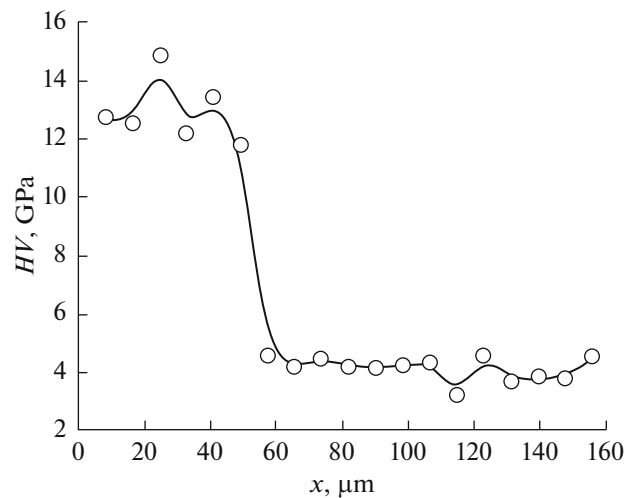
increase in the microhardness of the surface layer of steel regardless of the mode of treatment. The maximum microhardness value of the surface layer of steel was obtained in the case of specimens modified according to mode 1. Comparing the results of elemental and phase composition of the modified layer in Fig. 2 with the results of mechanical tests (Table 1), it can be stated that the maximum hardness of the surface layer of steel corresponds to the maximum concentration in the boron layer and the maximum relative content of titanium borides TiB and TiB<sub>2</sub>.

HIPE irradiation of a steel surface exposed to electroexplosive annealing with titanium and boron (modes 1 and 7) results in a decrease in the microhardness of the modified layer. During complex treatment according to modes 4 and 6, microhardness of the material is superior to that of steel in the state after EPA. The highest microhardness values, which are seven times as large as that of steel in the initial state, are achieved in the specimen modified according to mode 6. It should be noted that this mode of modification is characterized by the highest boron content in the surface layer (Fig. 2a, mode 6), which is formed exclusively by titanium borides (TiB and TiB<sub>2</sub>) and intermetallide (TiFe<sub>2</sub>).

Tribological characteristics (wear parameter (the value inverse to wear resistance) and friction coefficient) of 12Kh18N10T steel was only measured in the case of specimens exposed to complex treatment. A high roughness of the surface of the specimens after EPA did not allow us to measure these characteristics of material correctly. As follows from the results of the studies, the wear resistance of the steel (the value inverse to wear coefficient  $k$ ) after complex treatment combining EPA with titanium and boron and subsequent irradiation with an HIPE beam amounts to maximum values in the specimen modified according to mode 6 and exceeds the wear resistance of initial steel by a factor of more than nine.

In the case of the 12Kh18N10T steel specimen exposed to complex treatment according to mode 6, the microhardness profile was plotted (Fig. 3). It is clear that the thickness of the strengthened layer amounts to 60  $\mu\text{m}$ , while the layer hardness remains constant along the thickness.

It is evident that high strength and tribological characteristics of modified steel are caused by the structural-phase state of the material. The structural morphology of the surface layer of steel was investigated using transmission electron diffraction microscopy of thin foils [25–27]. The foils were prepared using ionic necking of the plates cut perpendicular to the surface of modification. Such an arrangement of foil allows one to analyze the state of material at various controlled distances from the surface of the specimen. An intrinsic image of the structure of the steel formed at various distances from the surface of treatment is given in Fig. 4.

**Fig. 3.** Microhardness profile of a 12Kh18N10T steel sample subjected to complex treatment using mode 6.

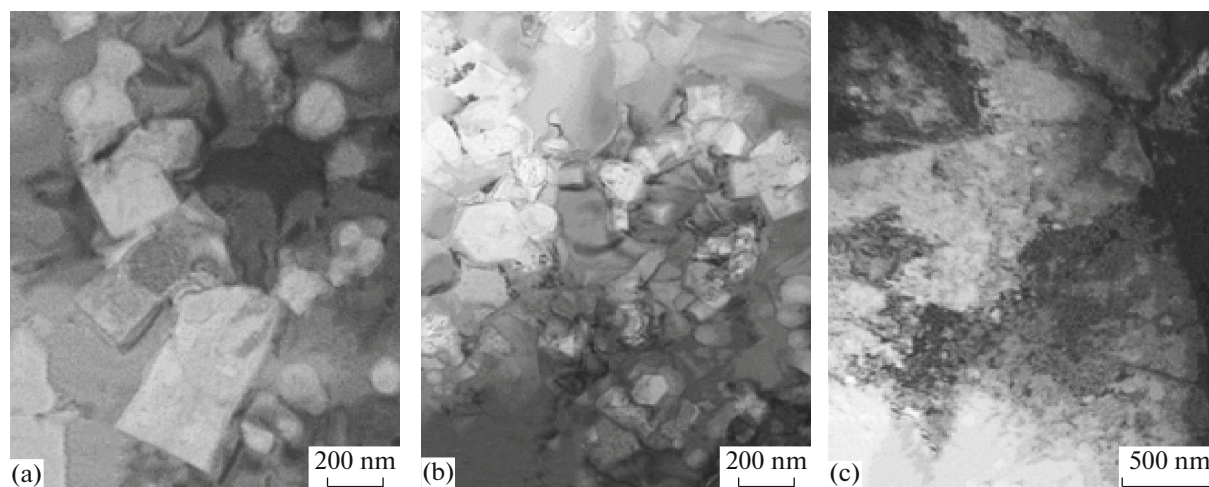


**Fig. 4.** Structure of 12Kh18N10T steel after complex treatment: (a) layer adjacent to the sample surface; (b) layer at nearly 40 microns depth; (c) layer at nearly 60 microns depth.

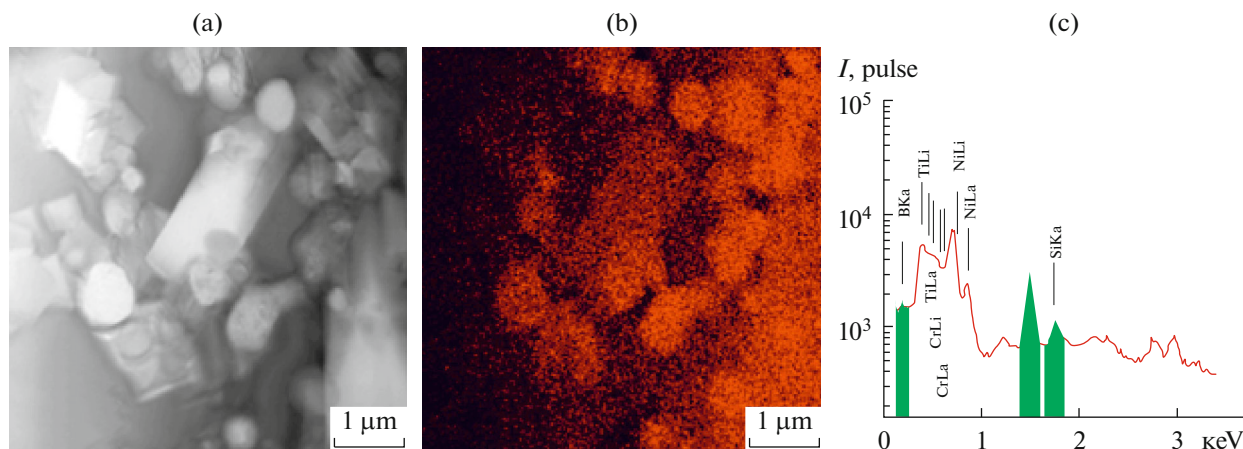


**Fig. 5.** Results of X-ray microspectral analysis of the modified layer of 12Kh18N10T steel (layer adjacent to the modifying surface was analyzed): (a) bright field; (b) image obtained in symptomatic X-ray radiation of titanium atoms; (c) fragment of energy spectra obtained from the foil piece shown in pos. (a) (layer adjacent to the modifying surface was analyzed).

It could be seen that the submicro-nanocrystalline structure is formed as a result of treatment in the surface layer of steel, in which the sizes of crystallites vary in the range from tens to hundreds of nanometers (Figs. 4a, 4b). The layer thickness with such a structure is less than 60  $\mu\text{m}$ . At large distances from the surface of the specimen, a polycrystalline structure is revealed, which is intrinsic for steel in the initial state (Fig. 4c).

The elemental composition of the modified layer was studied using X-ray microanalysis of thin foils (mapping method [23]). Results of the studies (Fig. 5) indicate a nonuniform distribution of alloying elements in the surface layer of steel. The domains

enriched and depleted with titanium could be detected (Figs. 5a, 5b).

The presence of boron atoms in the surface layer of steel using the mapping method is weakly detected. The results of X-ray microanalysis represented in the form of energy spectra (Fig. 5c) are more conclusive. These studies showed that the concentration of boron in the surface layer varies nonmonotonously amounting to the maximum value (nearly 19 at %) at a distance of 10–15  $\mu\text{m}$  from the alloying surface.

Analysis of the microelectronograms and use of dark-field images allows one to visualize the phases in steel [25–30]. An example of such an analysis is given in Fig. 6, which shows the images of  $\text{TiB}_2$  (Fig. 6c) and

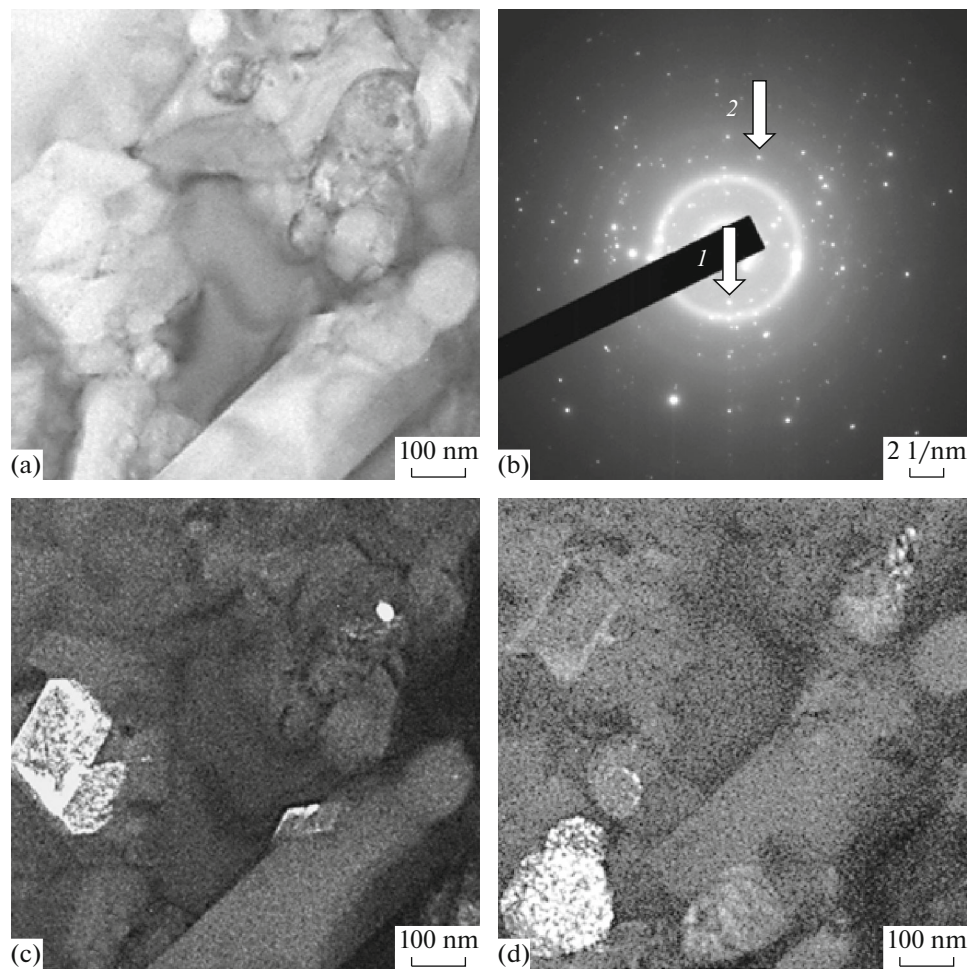


**Fig. 6.** Electron-microscopic image of 12Kh18N10T steel structure after complex treatment: (a) bright field; (b) microelectron diffraction pattern; (c, d) dark field obtained in the reflex of [100]  $\text{TiB}_2$  and [220]  $\text{TiB}$ ; at pos. c; arrows indicate reflexes in which a dark field is obtained (reflex 1—pos. c; reflex 2—pos. d) (layer adjacent to the modified surface was analyzed).

$\text{TiB}$  crystallites (Fig. 6d). The size of crystallites varies in a broad range from 30 to 200 nm.

## CONCLUSIONS

EPA of steel with titanium and boron has resulted in the formation of a surface layer possessing a multi-phase submicro-nanocrystalline structure, which is characterized by the presence of micropores, microcracks, and microcraters. It has been shown that the phase composition of the surface layer of steel is determined by the titanium-to-boron mass ratio upon electroexplosive alloying. It has been suggested that EPA with the parameters chosen in this study is accompanied not only by alloying of steel, but also the formation of thin coating enriched with titanium and boron atoms. It has been determined that the microhardness of the modified layer is governed by the mass fraction of titanium borides in the surface layer and could

exceed the microhardness of steel in the initial (before electroexplosive alloying) state by a factor of more than 18.

It has been determined that the complex treatment of the surface of high-chromium 12Kh18N10T stainless steel combining EPA with titanium and boron and subsequent irradiation with high-intense pulsed electron beam provides the formation of multi-phase submicro-nanocrystalline surface layers that is up to 60  $\mu\text{m}$  in thickness. The modes of complex treatment, which result in the formation of the surface layer containing exclusively titanium borides and intermetallide based on titanium and iron have been determined. The maximum (up to 82 wt %) content of titanium borides is observed upon treatment of steel according to the mode with the mass of boron powder in the sample of  $m_{\text{Ti}}/m_{\text{B}} = 5.202$ . With a decrease in the mass of boron powder, the relative content of borides in the surface layer of steel decreases.

Microhardness and wear resistance of the surface layer of 12Kh18N10T steel modified through complex treatment combining EPA with boron and titanium atoms and subsequent irradiation with a HIPE beam exceeds the microhardness of the material in initial state by the factor of more than seven, while wear resistance increases by the factor of more than nine.

#### FUNDING

The study was financially supported by grants of the Russian Science Foundation (project no. 18-79-00013 (experiments on electrical explosive alloying) and project no. 19-19-00183 (electron microscopy)).

#### REFERENCES

- Shulga, A.V., A comparative study of the mechanical properties and the behavior of carbon and boron in stainless steel cladding tubes fabricated by PM HIP and traditional technologies, *J. Nucl. Mater.*, 2013, vol. 434, nos. 1–3, pp. 133–140.
- Ma, S. and Zhang, J., Wear resistant high boron cast alloy—A review, *Rev. Adv. Mater. Sci.*, 2016, vol. 44, no. 1, pp. 54–62.
- Zhang, J., Gao, Y., Xing, J., Ma, S., Yi, D., Liu, L., and Yan, J., Effects of plastic deformation and heat treatment on microstructure and properties of high boron cast steel, *J. Mater. Eng. Perform.*, 2011, vol. 20, no. 9, pp. 1658–1664.
- Saha, R. and Ray, R.K., Development of texture, microstructure, and grain boundary character distribution in a high-strength boron-added interstitial-free steel after severe cold rolling and annealing, *Metall. Mater. Trans. A*, 2009, vol. 40, no. 9, pp. 2160–2170.
- Saha, R. and Ray, R.K., Microstructural and textural changes in a severely cold rolled boron-added interstitial-free steel, *Scr. Mater.*, 2007, vol. 57, no. 3, pp. 841–844.
- He, L., Liu, Y., Li, J., and Li, B.H., Effects of hot rolling and titanium content on the microstructure and mechanical properties of high boron Fe–B alloys, *Mater. Des.*, 2012, vol. 36, no. 4, pp. 88–93.
- Liu, Y., Li, B.H., Li, J., He, L., Gao, S.J., and Nieh, T.G., Effect of titanium on the ductilization of Fe–B alloys with high boron content, *Mater. Lett.*, 2010, vol. 64, no. 11, pp. 1299–1301.
- Samsonov, G.V., Markovskii, L.Ya., Zhigach, A.F., and Valyashko, M.G., *Bor. Ego soedineniya i splavy* (Boron Compounds and Alloys), Samsonov, G.V., Ed., Kiev: Akad. Nauk UkrSSR, 1960.
- Ren, X., Fu, H., Xing, J., and Yi, Y., Effect of solidification rate on microstructure and toughness of Ca–Ti modified high boron high speed steel, *Mater. Sci. Eng., A*, 2019, vol. 742, pp. 617–627.
- Gribkov, V.A., Grigor'ev, F.I., Kalin, B.A., and Yakushin, V.L., *Perspektivnye radiatsionno-puchkovye tekhnologii obrabotki materialov. Uchebnik* (Prospective Radiation-Beam Technologies for Materials Processing: Manual), Moscow: Kruglyi Stol, 2001.
- Koval', N.N. and Ivanov, Yu.F., Nanostructuring of surfaces of metaloceramic and ceramic materials by electron-beams, *Russ. Phys. J.*, 2008, vol. 51, no. 5, pp. 505–516.
- Poate, J.M., Foti, G., and Jacobson, D.C., *Surface Modification and Alloying: By Laser, Ion, and Electron Beams*, New York: Springer, 1983.
- Shulov, V.A., Paikin, A.G., Novikov, A.S., et al., *Sil'notochnye elektronnye impul'snye puchki dlya aviatsionnogo dvigatelestroeniya* (High-Voltage Electronic Pulsed Beams for Aircraft Engines), Shulov, V.A., Novikov, A.S., and Engel'ko, V.I., Eds., Moscow: Artek, 2012.
- Kadyrzhanov, K.K., Komarov, F.F., Pogrebnyak, A.D., et al., *Ionno-luchevaya i ionno-plazmennaya modifikatsiya materialov* (Ion-Beam and Ion-Plasma Modification of Materials), Moscow: Mosk. Gos. Univ., 2005.
- Uglov, V.V., Cherenda, N.N., Anishchik, V.M., Ashtashinskii, V.M., and Kvasov, N.T., *Modifikatsiya materialov kompressionnymi plazmennymi potokami* (Modification of Materials by Compression Plasma Flows), Minsk: Bel. Gos. Univ., 2013.
- Budovskikh, E.A., Martusevich, E.V., Nosarev, P.S., Gromov, V.E., and Sarychev, V.D., *Osnovy tekhnologii obrabotki poverkhnosti materialov impul'snoi geterogennoi plazmoi* (Theoretical Fundamentals of Materials Surface Treatment by Pulsed Heterogeneous Plasma), Novokuznetsk: Sib. Gos. Ind. Univ., 2002.
- Bagautdinov, A.Ya., Budovskikh, E.A., Ivanov, Yu.F., and Gromov, V.E., *Fizicheskie osnovy elektrovzryvnogo legirovaniya metallov i splavov* (Physical Fundamentals of Electroexplosive Alloying of Metals and Alloys), Novokuznetsk: Sib. Gos. Ind. Univ., 2007.
- Konovalov, S., Gromov, V., and Ivanov, Yu., Multilayer structure of Al–Si alloy after electro-explosion alloying with yttrium oxide powder, *Mater. Res. Express*, 2018, vol. 5, no. 11, art. ID 116520.
- Romanov, D.A., Gromov, V.E., Budovskikh, E.A., and Ivanov, Yu.F., Regularities of structural phase states formation on surface of metals and alloys during electroexplosive alloying, *Usp. Fiz. Met.*, 2015, vol. 16, no. 2, pp. 119–157.
- Struktura, fazovyi sostav i svoystva poverkhnostnykh sloev titanovykh splavov posle elektrovzryvnogo legirovaniya i elektronno-puchkovoi obrabotki* (Structure, Phase Composition and Properties of Surface Layers of Titanium Alloys after Electroexplosive Alloying and Electron-Beam Processing), Gromov, V.E., Ivanov, Yu.F., and Budovskikh, E.A., Eds., Novokuznetsk: Inter-Kuzbass, 2012.
- Sorokin, V.G., Volosnikova, A.V., Vyatkin, S.A., et al., *Marochnik stalei i splavov* (Grade Guide of Steels and Alloys), Sorokin, V.G., Ed., Moscow: Mashinostroenie, 1989.
- Rotshtein, V., Ivanov, Yu., and Markov, A., Surface treatment of materials with low-energy, high-current electron beams, in *Materials Surface Processing by Directed Energy Techniques*, Pauleau, Y., Ed., Amsterdam: Elsevier, 2006, pp. 205–240.

23. Krishtal, M.M., Yasnikov, I.S., Polunin, V.I., Filatov, A.M., and Ul'yanenkov, A.G., *Skanirovuyushchaya elektronnaya mikroskopiya i rentgenospektral'nyi analiz v primerakh prakticheskogo primeneniya* (Scanning Electron Microscopy and X-Ray Spectral Analysis in Practice), Krishtal, M.M., Ed., Moscow: Tekhnosfera, 2009.
24. *Diagrammy sostoyaniya dvoynykh metallicheskih sistem: Spravochnik* (State Diagrams of Binary Metal Systems: Handbook), Lyakishev, N.P., Ed., Moscow: Mashinostroenie, 1996, vol. 1.
25. Utevsii, L.M., *Difraktsionnaya elektronnaya mikroskopiya v metallovedenii* (Diffraction Electron Microscopy in Metal Science), Moscow: Metallurgiya, 1973.
26. Tomas, G. and Goringe, M.J., *Transmission Electron Microscopy of Materials*, New York: Wiley, 1979.
27. Andrews, K.W., Dyson, D.J., and Keown, S.R., *Interpretation of Electron Diffraction Patterns*, London, 1968.
28. *Transmission Electron Microscopy Characterization of Nanomaterials*, Kumar, C.S.S.R., Ed., New York: Springer, 2014.
29. Williams, D.B. and Carter, C.B., *Transmission Electron Microscopy: A Textbook for Materials Science*, Berlin: Springer, 2016.
30. Egerton, R.F., *Physical Principles of Electron Microscopy*, Berlin: Springer, 2016.

*Translated by A. Muravev*